

## Short-Wavelength Instability in a Linear Array of Vortices

O. Cardoso, H. Willaime, and P. Tabeling

*Laboratoire de Physique Statistique, 24 rue Lhomond, 75231 Paris, France*

(Received 5 April 1990)

The temporal instabilities of a linear array of vortices are studied experimentally; a short-wavelength instability is observed. The results are compared to a one-dimensional model of coupled nonlinear oscillators, leading to excellent agreement.

PACS numbers: 47.25.Qv, 05.70.Jk

The transition to spatiotemporal chaos is a problem of great current interest. Because of the large number of possible routes leading to weak turbulence, many studies are devoted to systems of low dimension. Spatiotemporal complexity is found in one-dimensional models such as those derived from Kuramoto-Shivashinsky<sup>1-3</sup> or Ginzburg-Landau equations.<sup>4</sup> Recently, the concept of one-dimensional pattern evolution to turbulence has been tested experimentally.<sup>5-7</sup>

The aim of this Letter is to report the investigation of a new system—a linear array of vortices. We will show that, from the dynamical point of view, it belongs to the class of one-dimensional systems. We report here the observation, prior to the onset of chaos, of a new short-wavelength instability, which, to the best of our knowledge, has not been observed earlier in unidimensional extended systems.

The experimental system is similar to that used in previous studies.<sup>8,9</sup> The cell is an open rectangular container, 350 mm long, 50 mm high, and 40 mm wide, machined out of Plexiglas. The working fluid, which is a normal solution of sulfuric acid, resides in a groove, 300 mm long, 20 mm wide, and 2 mm deep, machined in the bottom plate of the cell. Throughout the experiment, the thickness of the fluid layer is maintained at 2 mm, so that its free surface is flat at rest. Just below the fluid layer, a line of permanent magnets is formed; each individual magnet is a samarium cobalt parallelepiped, of dimensions  $5 \times 8 \times 3$  mm. They are put together to form a line of alternating poles. The vertical component of the resulting magnetic field, within the liquid layer, is a periodic function—roughly sinusoidal—of the coordinate along the lattice, with a zero mean value, and an amplitude of 0.3 T. A steady electric current  $I$  is driven longitudinally through the electrolyte; it interacts with the magnetic field to produce the flow.

For quantitative analysis, we use a shadowgraph technique, which is based on the fact that the free surface of the liquid is deflected by the rotation of the vortices. We thus form the image of the perturbed surface of the fluid by using a system of two confocal lenses, characterized by lateral magnifications ranging from  $\frac{1}{15}$  to  $\frac{1}{50}$ . This method allows for visualizing the separatrices between vortices as light lines. We further digitize the image and

track the position of such lines. In the time-dependent regimes, the corresponding ratio of signal to noise is about 40 dB.

At low currents, the basic state of flow is a linear array of counterrotating vortices of homogeneous size. As the electric current is increased above a first threshold value, the vortices cease to have a uniform size along the lattice axis: Half of them become larger at the expense of the others which decrease.<sup>8</sup> As  $I$  is increased further, the small vortices disappear and we end up with a system of stationary corotating vortices, with a size twice as large as that in the basic state. We denote this state by “state +.”

The corresponding images of the free surface, obtained by using the shadowgraph method, are shown in Fig. 1, for different values of the length of the system. The white lines correspond to the separatrices between each

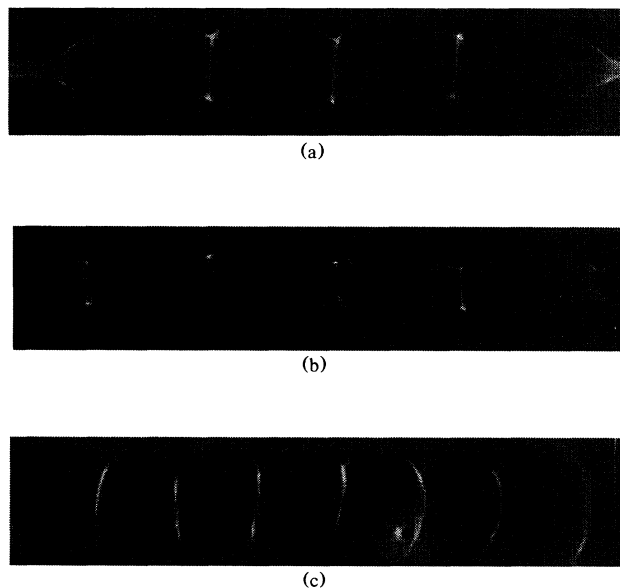


FIG. 1. Shadowgraph pictures of the free surface of linear arrays of vortices, for several values of the number of corotating vortices; all the pictures are obtained for  $I \sim 12$  mA. (a) Three corotating vortices; (b) five corotating vortices; (c) seven corotating vortices.

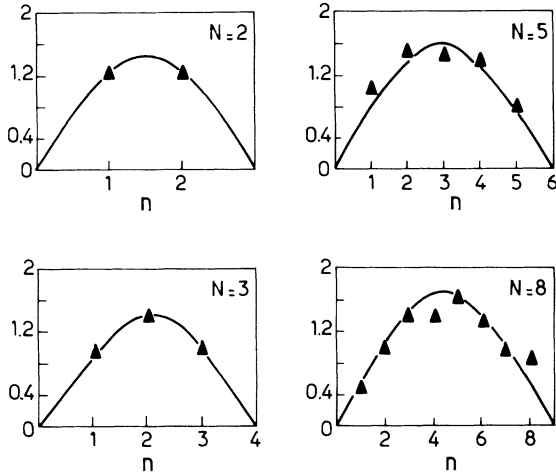


FIG. 2. Oscillation amplitudes of the optical mode along the lattice, for various values of its length ( $N$  denotes the number of separatrices). On the ordinate axis, the units are arbitrary. The solid lines are calculated by using Eq. (1).

pair of corotating vortices. In state  $+$ , the separatrices are stationary. Above a well defined threshold  $I_0$  (which depends on the size of the system), state  $+$  becomes unstable and the positions of the separatrices undergo monoprotic oscillations. By investigating the characteristics of the system close to the instability point, we find that the bifurcation from state  $+$  to the time-dependent state is a supercritical Hopf bifurcation. This result holds for all the systems which have been studied, i.e., including from two to ten corotating vortices. Concerning the spatial structure of the oscillating mode, we observe that it is in the form of an optical mode; i.e., the separatrices oscillate out of phase with their neighbor.

In the present experiment, the lattices are of finite size. End effects induce a modulation of period  $N + 1$  for the amplitude of the oscillation along the lattice (see Fig. 2). One can then define a dimensionless wave number associated with the optical model by the following expression:

$$k = \pi + 2\pi/(N + 1),$$

where  $N$  is the number of separatrices in the lattice.

Following these lines, the marginal stability and the dispersion curves of the system are obtained by plotting, respectively, threshold values  $I_0$  and frequency  $f_0$  of the optical mode as a function of wave number  $k$ . The two curves are shown in Fig. 3.

A secondary instability of the system appears upon the increase of the control parameter  $I$  above a new threshold. Figure 4 represents the state of flow after the onset of this instability, for various sizes of the lattice. The amplitudes of oscillation cease to be smoothly modulated in space, and a shorter-scale structure is visible. The corresponding perturbation tends to increase the amplitude of oscillation of half of the separatrices at the ex-

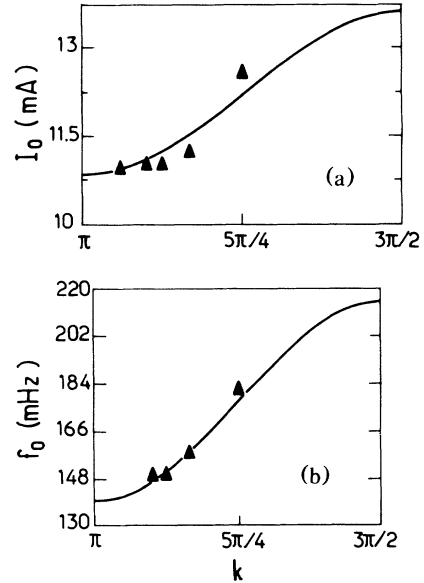


FIG. 3. (a) Marginal stability diagram; (b) dispersion relation. The solid lines are determined by using Eq. (1).

pense of their nearest neighbors. This secondary instability is observed for any value of the length of the system. The nature of this bifurcation is clearly supercritical for lattices of moderate sizes, i.e., up to five corotating vortices. For larger sizes, some irreversibility is observed, and it becomes more difficult to characterize the transition.

Upon further increase of the control parameter, a new state appears, whose nature depends on the length of the system. For moderately large lattices, the new state is a quasiperiodic regime, with two frequencies, while for sys-

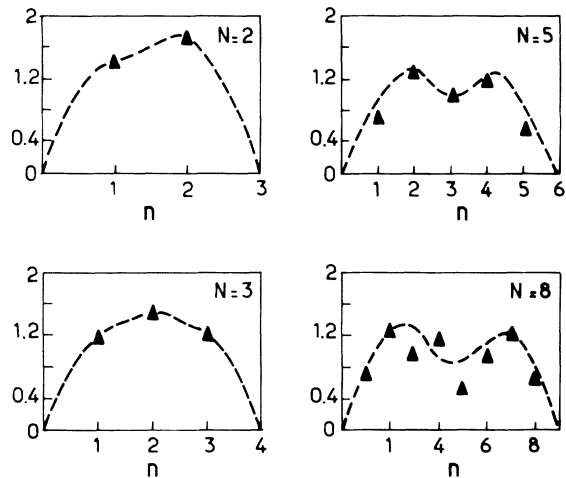


FIG. 4. Oscillation amplitudes of the optical mode perturbed by the short-wavelength mode, for various sizes of the lattice. The dashed lines correspond to typical amplitude envelopes found by using Eq. (1).

tems of larger sizes, the new state is a chaotic regime. These transitions are summarized in the phase diagram of Fig. 5(a).

The physical origin of the first mode of oscillation observed above  $I_0$  is presumably a shear instability which germinates in localized regions between the corotating vortices. The corresponding bifurcation is direct. It is then tempting to model the system as a chain of coupled nonlinear Hopf oscillators. Restricting ourselves to nearest-neighbor coupling, using reflectional symmetry and translational time invariance, one can write down, to the lowest order, the following model for our system:

$$\begin{aligned} \partial W_n / \partial t = & \mu(1 + ic_0)W_n - (1 + ic_2)W_n |W_n|^2 \\ & + \varepsilon(1 + ic_1)(W_{n-1} + W_{n+1}) \\ & - (c_3 + ic_4)W_n(|W_{n-1}|^2 + |W_{n+1}|^2), \end{aligned} \quad (1)$$

in which  $W_n$  is the complex amplitude of the  $n$ th oscillator,  $t$  is dimensionless time, and  $\mu$ ,  $\varepsilon$ ,  $c_0$ ,  $c_1$ ,  $c_2$ ,  $c_3$ , and  $c_4$  are real coefficients. Models similar to Eq. (1), but restricted to linear couplings, have been studied by Kuramoto.<sup>10</sup>

At the transition point, the most unstable mode is either an acoustical mode (for  $\varepsilon > 0$ ), where all the oscillators are in phase, or an optical mode (for  $\varepsilon < 0$ ), where each oscillator is out of phase with respect to its nearest neighbors. Since the temporal phase of such modes is defined only through an arbitrary constant, one can look for the instability which breaks the corresponding translation invariance. The calculation is formally similar to that of the Benjamin-Feir instability, and the results shown herein have been obtained for the case of infinite chains. The basic state is assumed to be the optical mode and the perturbed state reads

$$W_n = (A_0 + a_0 e^{i\delta n}) e^{i(\omega t + n\pi)}, \quad (2)$$

in which  $A_0$  and  $\omega$  are the amplitude and wave number

of the basic state, and  $a_0$  and  $\delta$  are the amplitude and wave number of the perturbation. Performing linear stability analysis, we find that the stability of the system essentially depends on a quantity  $\Delta(\delta)$  whose expression is

$$\Delta(\delta) = 1 + c_1 c_2 + 2 \cos \delta (c_3 + c_1 c_4). \quad (3)$$

A mode of wavelength  $\delta$  is unstable if  $\Delta(\delta)$  is negative; otherwise it is stable. Long-wavelength instabilities appear just above the primary instability point  $\mu = 2\varepsilon$  when  $\Delta(0)$  is negative. In this case, the resulting instability is similar to the Benjamin-Feir instability. A new situation appears when  $\Delta(0)$  is positive and  $\Delta(\pi)$  negative. In this case, the system is unstable against short wavelengths  $\delta = \pi$  at a finite distance from the primary instability point. The perturbed state is monophasic in time and its spatial structure is such that the amplitudes and phases of oscillation cease to be uniform along the lattice: Half of them are larger than their immediate neighbor.

We now proceed to the measurement of the coefficients of Eq. (1), using a strategy somewhat similar to that of a recent study.<sup>11</sup> The separatrices are labeled from 1 to  $N$  along the lattice and the order parameter  $W_n$  is understood as related to the temporal behavior of the  $n$ th separatrix. By investigating the transient behavior of the system close to  $I_0$ , for  $N=1$  and 2, we find the following values for the coefficients of Eq. (1):  $c_0 \approx 2.1$ ,  $c_1 \approx -4.3$ ,  $c_2 \approx -0.2$ ,  $c_3 \approx -0.08$ ,  $c_4 \approx -1.2$ ,  $\varepsilon \approx -0.05$ , and  $\mu = (I - I_c)/I_c$ , where  $I_c \approx 12.1$  mA. The corresponding marginal stability and dispersion curves are plotted in Fig. 3.

Using these values, one can further determine the nature of the secondary instability of the system, in the ideal case where the line of vortices is infinite, by computing  $\Delta(\delta)$ . We find that the system is stable to long wavelengths, and unstable against short-wavelength perturbations  $\delta = \pi$ . The corresponding instability has precisely the form found in the experiment.

These theoretical results are in agreement with a numerical study of Eq. (1), where the lattice is supposed to have perfectly reflecting ends; integration is performed by using the fourth-order Runge-Kutta method. The phase diagram calculated with the preceding values of the coefficients is shown in Fig. 5(b). There is a large domain where the optical mode is stable. This domain is limited from below by the marginal stability curve and from above by the short-wavelength instability discussed previously. In the upper region of the diagram, the system becomes either quasiperiodic (for lattices of moderate sizes) or chaotic (for large systems). Such results are in remarkable agreement with the experiment: The phase diagrams of Figs. 5(a) and 5(b) show striking similarities.

We therefore find a good agreement between the model and the experiment; this shows, at least, that our sys-

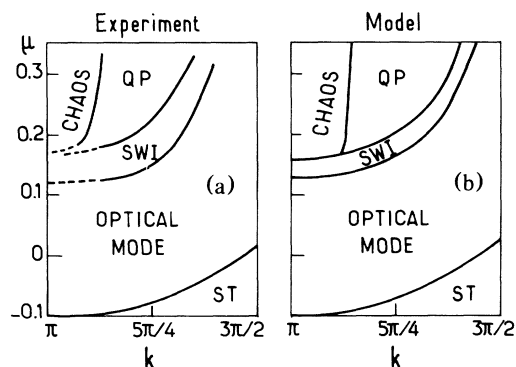


FIG. 5. Phase diagrams of the system. (a) Experiment; (b) Eq. (1), with the coefficients determined experimentally;  $\mu = (I - I_c)/I_c$ , where  $I_c \approx 12.1$  mA. The abbreviations are ST, stationary; SWI, short-wavelength instability; QP, quasiperiodic state.

tem, from a dynamical point of view, lives in a one-dimensional space. We have revealed the existence of a small-scale instability, which breaks the same symmetry as the Benjamin-Feir instability but is short wavelength (twice the lattice mesh) and appears at a finite distance from the primary instability point. This instability is related to the discrete nature of our system, and to the existence of nonlinear interactions between the oscillators [numerical computation of (1) shows that when  $c_3 = c_4 = 0$ , secondary instabilities appear at small wave number]. It would be interesting to compare such results with recent predictions concerning the secondary instabilities of periodic patterns.<sup>12</sup>

We are indebted to V. Croquette, D. Bensimon, and K. Sawada for illuminating discussions related to this experiment.

---

<sup>1</sup>Y. Kuramoto, *Prog. Theor. Phys. Suppl.* **64**, 346 (1978).

<sup>2</sup>G. I. Sivashinsky, *Acta Astronaut.* **4**, 1177 (1977).

<sup>3</sup>H. Chaté and P. Manneville, *Phys. Rev. Lett.* **54**, 112 (1987).

<sup>4</sup>P. Couillet, C. Elphick, and D. Repaux, *Phys. Rev. Lett.* **58**, 431 (1987).

<sup>5</sup>S. Ciliberto and P. Bigazzi, *Phys. Rev. Lett.* **60**, 286 (1988).

<sup>6</sup>M. Dubois, D. Da Silva, F. Daviaud, P. Bergé, and A. P. Petrov, *Europhys. Lett.* **8**, 135 (1989).

<sup>7</sup>M. Rabaud, S. Michalland, and Y. Couder, *Phys. Rev. Lett.* **64**, 184 (1990).

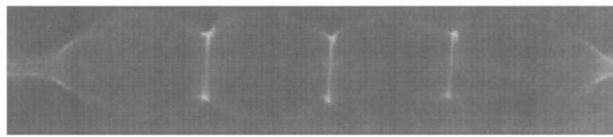
<sup>8</sup>P. Tabeling, S. Fauve, and B. Perrin, *Europhys. Lett.* **4**, 555 (1987).

<sup>9</sup>P. Tabeling, O. Cardoso, and B. Perrin, *J. Fluid Mech.* **213**, 511 (1990).

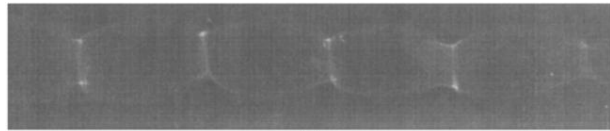
<sup>10</sup>Y. Kuramoto, *Chemical Oscillations, Waves and Turbulence* (Springer-Verlag, Heidelberg, 1984).

<sup>11</sup>V. Croquette and H. Williams, *Phys. Rev. A* **39**, 2765 (1989).

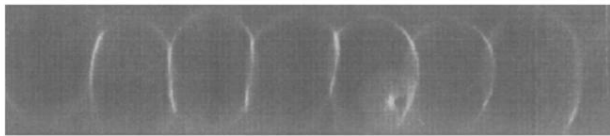
<sup>12</sup>P. Couillet and G. Ioss, *Phys. Rev. Lett.* **64**, 866 (1990).



(a)



(b)



(c)

FIG. 1. Shadowgraph pictures of the free surface of linear arrays of vortices, for several values of the number of corotating vortices; all the pictures are obtained for  $I \sim 12$  mA. (a) Three corotating vortices; (b) five corotating vortices; (c) seven corotating vortices.